

Axial Force Calculation of Passive Magnetic Bearing

Ana N. Vučković¹, Nebojša B. Raičević¹, Saša S. Ilić¹,
Slavoljub R. Aleksić¹, Mirjana T. Perić¹

Abstract: Axial magnetic force calculation between two ring permanent magnets is presented in the paper. One magnet is magnetized in radial direction while the other one is magnetized in axial direction. Configuration like this one resembles the one passive magnetic bearing has. Force calculation is performed using semi analytical approach based on fictitious magnetization charges and discretization technique. For comparison purposes, and in order to check preciseness of the method applied, Finite Element Method (FEM) results were used.

Keywords: Magnetic bearing, Magnetization charges, Magnetic force, Ring permanent magnet.

1 Introduction

Since permanent magnets have numerous applications, the need for the optimization leads to the development of calculation methods. Functionality of the devices that use permanent magnets greatly depends on the magnet material, magnetization and dimensions. One example of permanent magnet applications are magnetic bearings, as contactless suspension devices with various rotating and translational applications. They can act as axial or radial bearings depending on direction of the ring permanent magnet magnetization. Since Yonnet presented the first study concerning different permanent magnet configuration [1], many scientists around the World are dealing with this issue by carrying out various researches in order to determine the magnetic field of permanent magnets and the force between them accurately and efficiently. Although there are many different methods one could use in order to analyse permanent magnets, the fact is that Ampere's current model [2, 8] and the Coulombian approach [3, 4, 9] are the ones most frequently used.

Interaction force determination of magnetic bearing is presented in the paper. It is derived using the semi analytical method based on magnetization

¹University of Niš, Faculty of Electronic Engineering, Aleksandra Medvedeva 14, 18000 Niš, Serbia;
E-mails: ana.vuckovic@elfak.ni.ac.rs; nebojsa.raicevic@elfak.ni.ac.rs; sasa.ilic@elfak.ni.ac.rs;
slavoljub.aleksic@elfak.ni.ac.rs; mirjana.peric@elfak.ni.ac.rs

charges and discretization technique. Obtained expression is easily used in any programming environment and requires less than one second of run time on a personal computer.

2 Calculation method

Passive magnetic bearing that is considered in the paper is presented in the Fig.1. Upper magnet is uniformly magnetized in axial direction. Therefore, only fictitious surface magnetization charges

$$\eta_{m1} = \hat{n}\mathbf{M}_1, \quad (1)$$

exist on the bottom and the top bases of permanent magnet, because volume magnetization charges for uniform axial magnetization do not exist, [3, 5]. \hat{n} is the unit vector normal to surface.

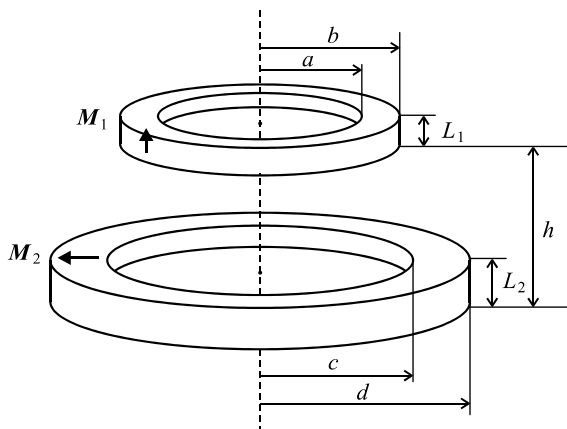


Fig. 1 – Passive magnetic bearing.

The lower magnet is magnetized in radial direction, [4, 6], therefore the fictitious magnetic charge density is composed of volume and surface charge density. Since the boundary condition for surface magnetization charges density has to be satisfied

$$\eta_{m2} = \hat{n}\mathbf{M}_2, \quad (2)$$

it is obvious that fictitious surface magnetization charges exist only on inner and outer cover of lower permanent magnet. Volume fictitious magnetization charges satisfy the following expression

$$\rho_m = -\text{div } \mathbf{M}_2 = -\frac{M_2}{r}. \quad (3)$$

The simplest way to calculate the interaction magnetic force is to discretize each permanent magnet into system of circular loops loaded with magnetic charges. The interaction force between two magnetized circular loops is determined first [5, 6]. Using results for the axial magnetic force between two circular loops, magnetic force of the considered configuration can be performed by summing the contribution of both magnets using uniform discretization technique.

Procedure for magnetic force determination is to discretize upper permanent magnet bases into system of N_{s1} segments (circular loops). The lower permanent magnet covers can be considered as a system of N_{s2} segments and its volume can be discretized into system of N_v^{tot} circular loops.

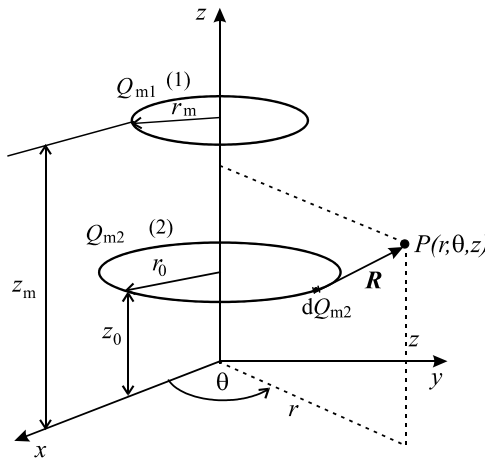


Fig. 2 – Two circular loops.

Magnetic force components between two circular loops, Fig. 2, derived in [6] are:

$$F_r = \mu_0 \frac{Q_{m1} Q_{m2}}{2\pi^2} \times \left(\frac{(r_m^2 - r_0^2 - (z_m - z_0)^2) E\left(\frac{\pi}{2}, k_0\right)}{2r_m \left((r_m - r_0)^2 + (z_m - z_0)^2 \right) \sqrt{(r_m + r_0)^2 + (z_m - z_0)^2}} \right. \\
 \left. + \frac{K\left(\frac{\pi}{2}, k_0\right)}{2r_m \sqrt{(r_m + r_0)^2 + (z_m - z_0)^2}} \right) = 0 \tag{4}$$

$$F_z = \mu_0 \frac{Q_{m1} Q_{m2}}{2\pi^2} \times \frac{(z_m - z_0) E\left(\frac{\pi}{2}, k_0\right)}{\left((r_m - r_0)^2 + (z_m - z_0)^2\right) \sqrt{(r_m + r_0)^2 + (z_m - z_0)^2}} = \quad (5)$$

$$= \mu_0 \frac{Q_{m1} Q_{m2}}{2\pi^2} F_{z_p}(r_0, r_m, z_0, z_m)$$

with elliptic integrals modulus $k_0^2 = \frac{4r_0 r_m}{(r_m + r_0)^2 + (z_m - z_0)^2}$.

The axial component of the force (5) presents interaction force between two magnetized circular loops.

Considering Fig. 3, it is obvious that, for both magnets, the following formulas are satisfied

$$\eta_{m1} = \hat{n}_1 \mathbf{M}_1 = M_1, \quad \eta_{m2} = \hat{n}_2 \mathbf{M}_1 = -M_1, \quad \eta_{m3} = \hat{n}_3 \mathbf{M}_2 = -M_2, \quad (6)$$

$$\eta_{m4} = \hat{n}_4 \mathbf{M}_2 = M_2 \quad \text{and} \quad \rho_m = -\text{div} \mathbf{M}_2 = -\frac{M_2}{r}.$$

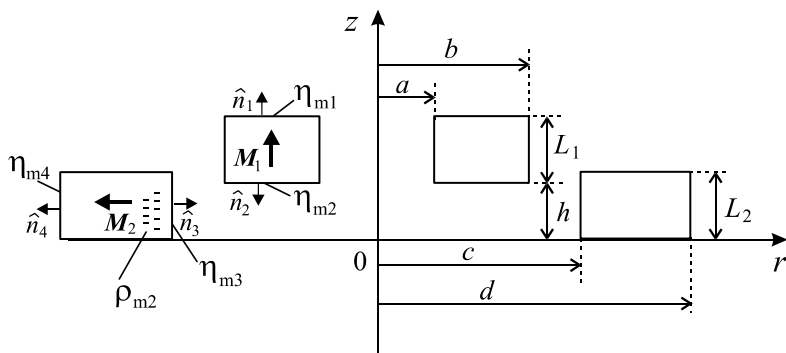


Fig. 3 – Distribution of surface and volume magnetic charges.

By taking into account the ring permanent magnet geometry, Fig. 4, the following parameters can be defined for segments of the upper magnet bases:

$$r_i = a + \frac{2i-1}{2N_{s1}}(b-a), \quad i = 1, 2, \dots, N_{s1},$$

$$z_{1i} = h, \quad i = 1, 2, \dots, N_{s1},$$

$$z_{2i} = h + L_1, \quad i = 1, 2, \dots, N_{s1},$$

and magnetization charges of the loops for lower and upper bases are

$$Q_{m1i} = -M_1 2\pi r_i \frac{b-a}{N_{s1}}, \quad i = 1, 2, \dots, N_{s1},$$

$$Q_{m2i} = M_1 2\pi r_i \frac{b-a}{N_{s1}}, \quad i = 1, 2, \dots, N_{s1}.$$

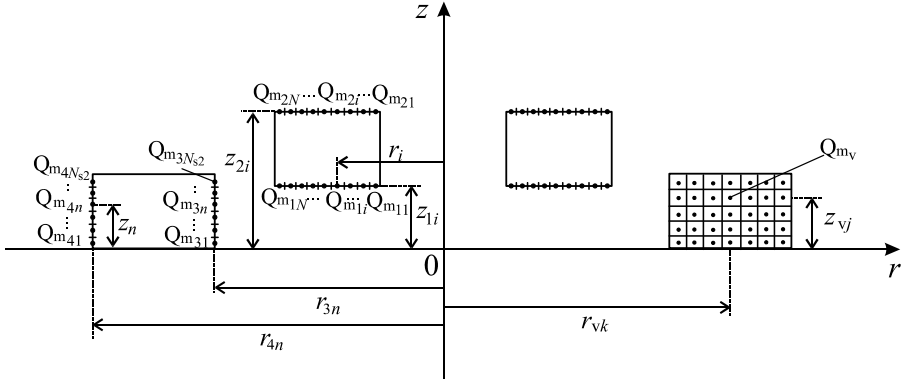


Fig. 4 – Discretizing model.

For the lower magnet the parameters for covers segments are

$$z_n = \frac{2n-1}{2N_{s2}} L_2, \quad n = 1, 2, \dots, N_{s2},$$

$$r_{3n} = c, \quad n = 1, 2, \dots, N_{s2},$$

$$r_{4n} = d, \quad n = 1, 2, \dots, N_{s2},$$

and loops magnetization charges of lower permanent magnet covers are

$$Q_{m3n} = -M_2 2\pi c \frac{L_2}{N_{s2}}, \quad n = 1, 2, \dots, N_{s2},$$

$$Q_{m4n} = M_2 2\pi d \frac{L_2}{N_{s2}}, \quad n = 1, 2, \dots, N_{s2},$$

where N_{s1} is segments number of each base of upper permanent magnet and N_{s2} is number of segments of each cover for lower ring permanent magnet. Therefore, the total number of surface segments for analysed system is $N_s^{\text{tot}} = N_{s1} + N_{s2}$.

Since the volume fictitious magnetization charges exist in lower magnet, the volume of magnet can be considered as systems of circular magnetized loops (Fig. 4) with parameters

$$z_{vj} = \frac{2j-1}{2N_{v3}}L_2, \quad j=1,2,\dots,N_{v1},$$

$$r_{vk} = c + \frac{2k-1}{2N_{v4}}(d-c), \quad k=1,2,\dots,N_{v2},$$

and magnetization charges of the loops are

$$Q_{mv} = Q_{m_{vn}} = -M_2 2\pi L_2 \frac{d-c}{N_{v1}N_{v2}}, \quad n=1,2,\dots,N_{v1}N_{v2},$$

where $N_v^{\text{tot}} = N_{v1} \cdot N_{v2}$ is the number of segments for lower ring permanent magnet volume.

Using results for interaction magnetic force between two circular loops (5), the interaction magnetic force between two ring permanent magnets can be obtained. It can be achieved by summing the contribution of lower ring covers and volume and the contribution of upper ring bases by using uniform discretization technique

$$F_z = F_{z13} + F_{z23} + F_{z14} + F_{z24} + F_{z1v} + F_{z2v}, \quad (7)$$

where $F_{z13} + F_{z23} + F_{z14} + F_{z24}$ is the force between circular magnetized loops (segments) of upper magnet bases and lower magnet covers (force between surface charges) and $F_{z1v} + F_{z2v}$ is the force between volume segments of lower magnet and surface segments of upper magnet.

Finally, interaction magnetic force between two ring permanent magnets is

$$F_z = \frac{\mu_0}{2\pi^2} \left(\sum_{i=1}^{N_{s1}} \sum_{n=1}^{N_{s2}} (Q_{m1i} Q_{m3n} F_{z_p}(r_{3n}, r_i, z_n, z_{1i}) + Q_{m2i} Q_{m3n} F_{z_p}(r_{3n}, r_i, z_n, z_{2i}) + \right. \\ \left. Q_{m1i} Q_{m4n} F_{z_p}(r_{4n}, r_i, z_n, z_{1i}) + Q_{m2i} Q_{m4n} F_{z_p}(r_{4n}, r_i, z_n, z_{2i})) + \right. \\ \left. \sum_{i=1}^{N_{s1}} \sum_{j=1}^{N_{v1}} \sum_{k=1}^{N_{v2}} (Q_{mv} Q_{m1i} F_{z_p}(r_{vk}, r_i, z_{vj}, z_{1i}) + Q_{mv} Q_{m2i} F_{z_p}(r_{vk}, r_i, z_{vj}, z_{2i})) \right). \quad (8)$$

3 Numerical Results

The results obtained for presented system, using semi analytical approach, are given graphically.

Presumption was that both permanent magnets are made of the same material and magnetized uniformly with same intensity, $M_1 = M_2 = M$, the upper one in axial and the lower one in radial direction. In order to save the calculation time, the number of segments is limited on $N_s^{\text{tot}} = N_v^{\text{tot}} = 100$,

because it is not necessary to take a greater number of segments to obtain a desired accuracy, as it is shown in **Table 1**.

Compared results for axial force with the finite element method (FEMM 4.2 software) [10] are given in **Table 2** for ring permanent magnets' parameters $c/L_2 = 3$, $d/L_2 = 4$, $L_1/L_2 = 1.0$ and $h/L_2 = 1.5$. Relative error of calculation compared with the finite element method is also presented in the table.

Table 1

Convergence of normalized levitation magnetic force versus number of segments.

$N_s^{tot} \backslash N_v^{tot}$	25	50	100	150	200	300
25	-0.486486	-0.486566	-0.486584	-0.486588	-0.486589	-0.486590
50	-0.486521	-0.486601	-0.486619	-0.486622	-0.486623	-0.486624
75	-0.486535	-0.486615	-0.486633	-0.486636	-0.486637	-0.486638
100	-0.486539	-0.486619	-0.486637	-0.486640	-0.486641	-0.486642
150	-0.486544	-0.486624	-0.486642	-0.486646	-0.486647	-0.486648
200	-0.486548	-0.486641	-0.486646	-0.486649	-0.486647	-0.486651
300	-0.486551	-0.486644	-0.486649	-0.486652	-0.486653	-0.486654

Table 2

Compared results for normalized interaction magnetic force versus a/L_2 and b/L_2 .

a/L_2	b/L_2	F_z^{nor}	F_z^{nor} (FEM)	Relative error [%]
1.0	2.0	0.095805	0.095665	-0.1463
1.5	2.5	0.414182	0.413885	-0.0717
2.0	3.0	1.096810	1.095936	-0.0797
2.5	3.5	1.398870	1.397204	-0.1192
3.0	4.0	0.217268	0.214446	-1.3159
3.5	4.5	-1.268150	-0.127006	0.1504
4.0	5.0	-1.324010	-1.325731	0.1298
4.5	5.5	-0.644149	-0.644430	0.0436
5.0	6.0	-0.227007	-0.227140	0.0585

To maximize the possibility of analysing axial force for the various parameters values, normalized axial force, $F_z^{nor} = F_z / (\mu_0 M^2 L_2^2)$, is presented in the figures. Fig. 5 presents axial magnetic force versus ratio h/L_2 for different air gap dimension $\delta/L_2 = c/L_2 - b/L_2$.

Axial magnetic force versus ratio h/L_2 , for different heights of permanent magnets, is presented in Fig. 6, while Fig. 7 shows interaction magnetic force versus ratio h/L_2 for different width of upper permanent magnet.

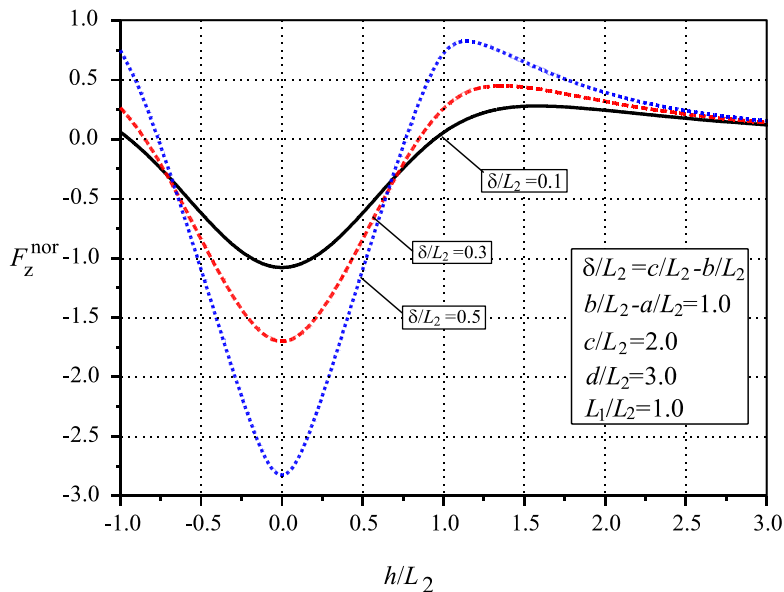


Fig. 5 – Axial magnetic force versus ratio h/L_2 for different air gap dimension.

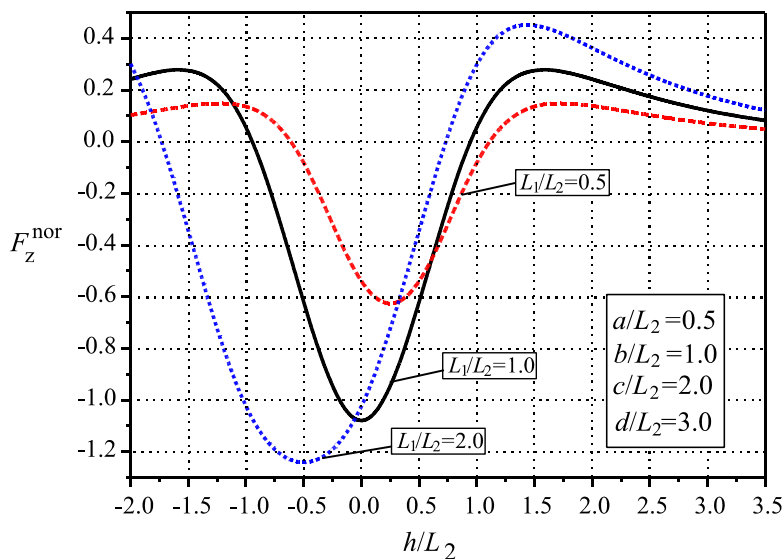


Fig. 6 – Axial magnetic force versus ratio h/L_2 for different heights of permanent magnets.

Considering previous two figures it can be concluded that as the normalised width and height of upper magnet increase, the absolute value of the axial force increases. But the compromise in dimensions of permanent magnets must be found since the costs of the magnets have to be taken in to account.

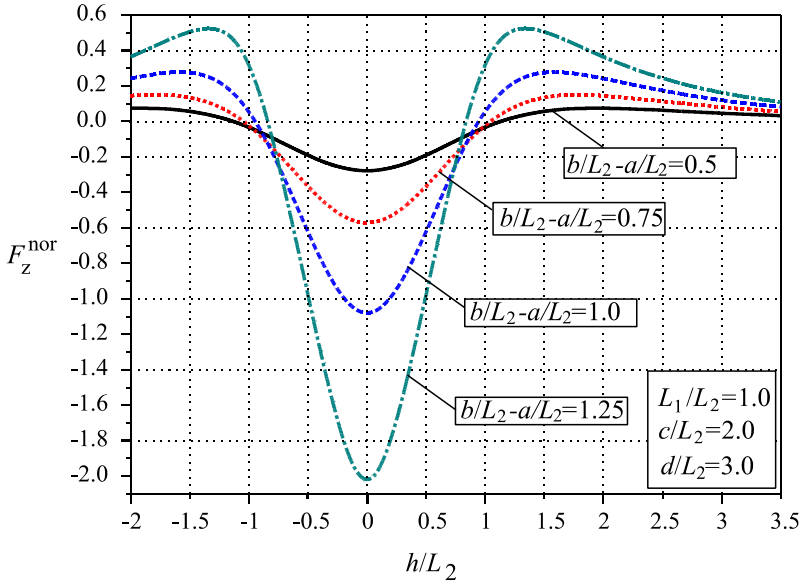


Fig. 7 – Axial magnetic force versus ratio h/L_2 for different width of upper permanent magnet.

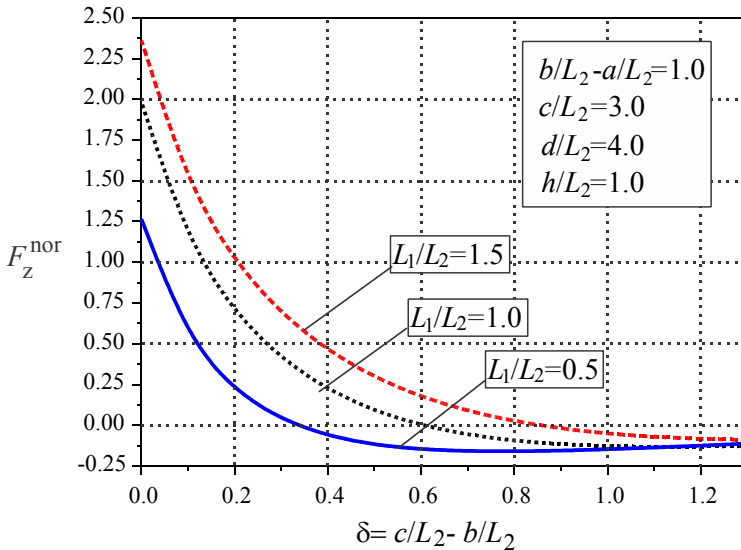


Fig. 8 – Axial magnetic force versus the air gap dimension.

Axial magnetic force versus air gap is shown in Fig. 8.

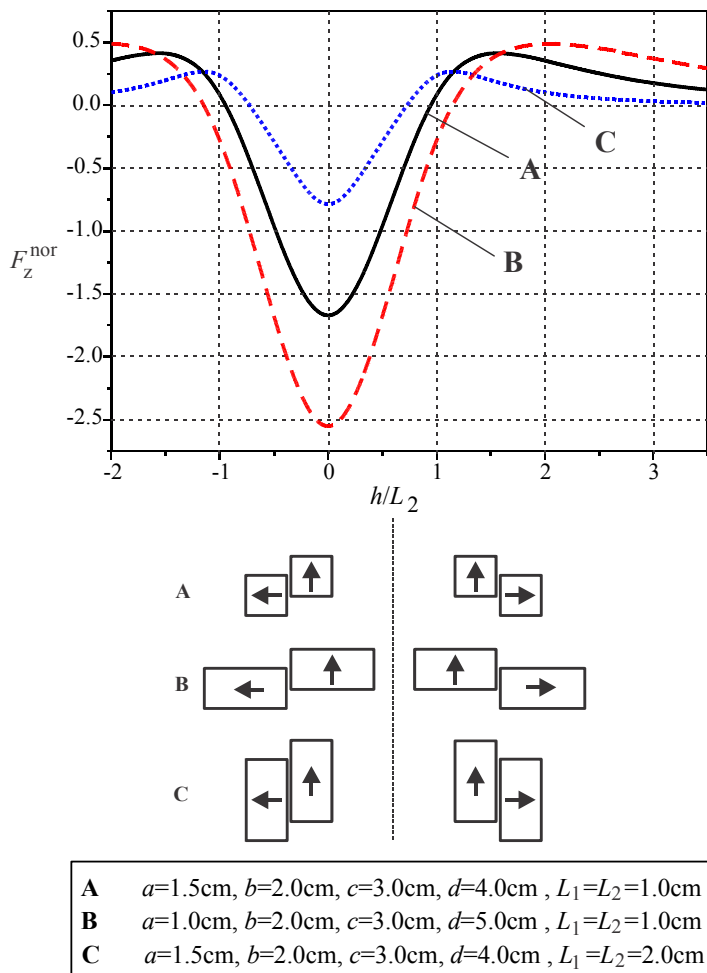


Fig. 9 – Axial magnetic force versus ratio h/L_2 for different configurations of magnetic bearing.

In order to find the optimal dimensions of permanent magnets, three different configurations are considered Fig. 9.

The first one consists of two ring magnets of square cross section (A). The second one consists of two ring magnets of rectangular cross section whose width is two times its height (B), and the third one consists of two magnets of rectangular cross section whose height is two times its width (C). Fig. 9 presents normalised axial force for presented configurations versus normalised axial displacement of inner permanent magnet h/L_2 .

4 Conclusion

Determination of the axial forces of radial passive magnetic bearing is presented. It is performed using magnetization charges and discretization technique. The derived algorithm is easily implemented in any standard computer environment and it enables rapid parametric studies of the interaction force what can be useful for magnetic bearing design as a primary component of great number of magnetic devices. The results of the presented approach are successfully confirmed using FEMM 4.2 software. Interaction forces calculation using presented approach for mentioned parameters is performed with Intel Core i5-2320 CPU Quad Core at 3GHz and 8GB RAM memory, 64-bit operating system and it took around 0.76 seconds of run time for one calculation. Interaction forces are also determined on the same computer using FEMM 4.2 software and the execution time was 5.6 minutes for about 2 million finite elements. Advantage of presented approach comparing to the FEM is its accuracy, simplicity and time efficiency since only complete elliptic integrals of the second kind are used and other additional integrations are avoided in this approach.

5 Acknowledgement

The work presented here was partly supported by the Serbian Ministry of Education and Science in the frame of the project TR 33008.

6 References

- [1] J. P. Yonnet: Passive Magnetic Bearings with Permanent Magnets, IEEE Transactions on Magnetics, Vol. 14, No. 5, Sept. 1978, pp. 803–805.
- [2] A. N. Vučković, S. S. Ilić, S. R. Aleksić: Interaction Magnetic Force Calculation of Ring Permanent Magnets Using Ampere's Microscopic Surface Currents and Discretization Technique, Electromagnetics, Vol. 32, No. 2, 2012, pp. 117–134.
- [3] R. Ravaut, G. Lemarquand, V. Lemarquand: Force and Stiffness of Passive Magnetic Bearings using Permanent Magnets. Part 1: Axial Magnetization, IEEE Transactions on Magnetics, Vol. 45, No. 7, July 2009, pp. 2996–3002.
- [4] R. Ravaut, G. Lemarquand, V. Lemarquand: Force and Stiffness of Passive Magnetic Bearings using Permanent Magnets. Part 2: Radial Magnetization, IEEE Transactions on Magnetics, Vol. 45, No. 9, Sept. 2009, pp. 3334–3342.
- [5] S. S. Ilić, A. N. Vučković, S. R. Aleksić: Interaction Magnetic Force Calculation of Axial Passive Magnetic Bearing using Magnetization Charges and Discretization Technique, 15th International IGTE Symposium on Numerical Field Calculation in Electrical Engineering, Graz, Austria, 17–19, Sept. 2012, pp. 300–305.
- [6] A. N. Vučković, N. B. Raičević, S. S. Ilić, S. R. Aleksić: Interaction Magnetic Force Calculation of Radial Passive Magnetic Bearing using Magnetization Charges and Discretization Technique, International Journal of Applied Electromagnetics and Mechanics, Vol. 43, No.4, 2013, pp. 311–323.

- [7] K. Bachovchin, J. Hoburg, R. Post: Magnetic Field and Forces in Permanent Magnet Levitated Bearings, IEEE Transactions on Magnetics, Vol. 48, No. 7, July 2012, pp. 2112–2120.
- [8] E. P. Furlani, S. Reznik, A. Kroll: A Three-Dimensional Field solutiOn for Radially Polarized Cylinders. IEEE Transactions on Magnetics, Vol. 31, No.1, 1995, pp. 844–851.
- [9] H. L. Rakotoarison, J.-P. Yonnet, B. Delinchant: Using Coulombian Approach for Modeling Scalar Potential and Magnetic Field of a Permanent Magnet with Radial Polarization, IEEE Transactions on Magnetics, Vol. 43, No. 4, 2007, pp. 1261–1264.
- [10] D. Meeker, Software package FEMM 4.2, <http://www.femm.info/wiki/>, Download (accessed 2 March 2007).